

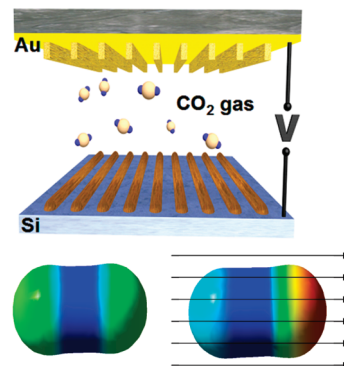
Splitting CO₂ with Electric Fields: A Computational Investigation

M. Calvaresi,^{*,†} R. V. Martinez,[‡] N. S. Losilla,[‡] J. Martinez,[‡] R. Garcia,[‡] and F. Zerbetto^{*,†}

[†]Dipartimento di Chimica "G. Ciamician", Universita' di Bologna, V. F. Selmi 2, 40126 Bologna, Italy, and [‡]Instituto de Microelectrónica de Madrid, CSIC, Isaac Newton 8, Tres Cantos, 28760 Madrid, Spain

ABSTRACT Quantum chemical calculations at the B3LYP/aug-cc-PVTZ level show that CO₂ can spontaneously break in the presence of an electric field above 40 V/nm. The energetics of the reaction was further assessed by single-point CCSD(T) calculations, which show that the electric field transforms the reaction from endothermic to exothermic. The rupture occurs when the potential energy curves of the singlet and triplet manifolds cross each other and is caused by the fast decrease of the energy of the lowest unoccupied molecular orbital. The process was present in recent experiments carried out with atomic force microscopy at room temperature in the presence of low-to-moderate voltages (*Appl. Phys. Lett.* **2010**, *96*, 143110). The simulation of the electric field-dependent infrared spectra show the process could be monitored spectroscopically since the symmetric CO stretch becomes infrared-allowed and downshifts in the presence of the field, while the bending acquires further intensity.

SECTION Molecular Structure, Quantum Chemistry, General Theory



External electric fields (EEFs) can affect a variety of chemical events including electron transfer reactions,^{1–4} charge transfer between surfaces,⁵ small-molecule–surface interactions,^{6,7} and electron transport in molecular devices.^{8–10} Oriented EFs can induce conformational changes and isomerization processes,¹¹ as well as chemical reactions that involve bond-formation and bond-breaking.^{12–16} This versatility can explain the growing interest in the use of EEFs to modulate chemical reactions, since it is possible, using oriented EEFs, to affect the regioselectivity and stereoselectivity of the reactions or enhance/decrease the rate of a reaction of several order of magnitude.^{12–16} EEFs change the energy landscape of chemical processes and thereby have an impact on the mechanism, rate, and selectivity of the reaction. Electric fields modify the molecular geometry, drastically alter the molecular electric dipole moments, and redistribute the electron density of molecular orbitals (MOs) as well as reduce the energy gap between frontier MOs.^{17–19}

The control and manipulation of electric fields at the nanoscale has enabled the emergence of a flexible atomic force microscope (AFM) nanolithography.²⁰ This nanolithography is based on the field-induced activation of molecules within a liquid meniscus. Different liquids such as water,²⁰ ethanol,²¹ octane,²² octene,²⁰ or hexadecane^{23,24} have been used. Very recently it was shown that the field-induced activation of liquid molecules can be extended to transform stable gases such as carbon dioxide to carbonaceous material.²⁵ The process exploits electric fields in the range of tens of volts per nanometer that can be generated with a nanoscale asperity to obtain the energy needed to convert carbon dioxide gas into a solid material. The process takes place at room temperature

and uses low-to-moderate voltages (~10–40 V). The activation of carbon dioxide can be performed with a single nanoscale asperity (in AFM experiments) or with a macroscopic surface patterned with billions of nanoscale asperities. The experimental field was qualitatively estimated to be up to 30 V/nm from the value of the applied voltage of 1–40 V. However, depending on the position of the CO₂ molecule with respect to the origin of the electric potential, the local field experienced by a CO₂ molecule can be greater or even much greater. The energy efficiency to transform a single carbon dioxide gas molecule to carbonaceous material is close to unity.²⁵

The high enthalpy of formation of carbon dioxide, ca. –4.1 eV (394 kJ/mol),²⁶ makes it chemically very stable. Of the several processes to activate the transformation of CO₂,^{27,28} one of the most important is probably the naturally occurring Calvin cycle. The Calvin cycle is the metabolic pathway used by photosynthetic organisms for carbon fixation where carbon enters in the form of CO₂ and leaves in the form of sugar. Other technological processes use a combination of catalysts, high temperature surfaces, and/or electrochemical induced reactions.²⁸ In general, however, it can be said that current technological approaches to activate carbon dioxide molecules are either costly in terms of energy consumption or lack universality.

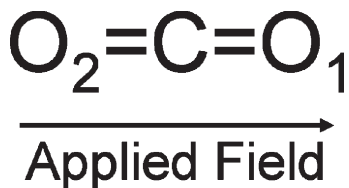
In this paper, quantum chemical calculations show how EEFs affect the molecular geometry and the electron density

Received Date: July 23, 2010

Accepted Date: October 21, 2010

Published on Web Date: October 29, 2010

Scheme 1. Orientation of Field Applied to CO₂ Molecule



of CO₂, change its properties, modify the potential energy surface of its dissociation, and shift the energy of the MOs, which ultimately leads to carbon dioxide splitting. We employ the Gaussian03²⁹ suite of programs to investigate the structural and electronic changes brought by the application of uniform static electric fields. Calculations are carried out using density functional theory (DFT) with Becke's three-parameter hybrid functional (B3)³⁰ combined with the electron-correlation functional of Lee, Yang, and Parr (LYP),³¹ abbreviated as the B3LYP³² method. Geometries were optimized using the aug-cc-PVTZ³³ basis set (triple- ζ basis set augmented with diffuse and polarization functions), which uses 46 basis functions [5s,4p,3d,2f] for C and O atoms. The flexibility provided by the polarization and diffuse functions is deemed crucial to describe the CO₂ response to EEFs. In the recent past, smaller basis sets, such as 6-311++G(2d,2p) that entail 27 basis functions per atom, have been employed for related investigations.^{12–14,17–19} All calculations use the Field keyword in Gaussian03,²⁹ which defines the EF axis, its direction, and magnitude. We have considered fields of magnitude 5, 10, 20, 30, and 40 V/nm, which appear in AFM nanolithography experiments to be able to split CO₂.²⁵ Vibrational frequencies were calculated, in the presence of fields, to confirm that the optimized structures are minima, to yield the IR spectrum perturbed by the applied field, and to calculate electrical polarizabilities. Single point CCSD(T) calculations were carried out on the optimized DFT geometries to obtain more accurate values of energy.

We examined the effect of electric fields of increasing strength on CO₂. We originally performed calculations with a variety of electric field orientations with respect to the molecular axis. Only the results for the field oriented along the axis are presented and discussed, since this configuration generates the most stable systems (Scheme 1).

The field polarizes the molecular wave function. To assess the accuracy of the computational model, one can compare experimental and calculated polarizabilities in the absence of the field (Table 1).

The molecular polarizability $\langle\alpha\rangle$ is 17.17 au³ versus an experimental value of 17.76,³⁵ the calculated value of α_{\parallel} is 26.024 au³ versus an experimental value of 27.250 au³,³⁵ while the calculated value of α_{\perp} is 12.750 au³ versus an experimental value of 13.018 au³. These values vouch for the accuracy of the model, also if compared to other high-level calculations.³⁶

Table 2 shows the optimized geometry together with other quantities. In the presence of the field, one of the C–O bonds, C–O₁, elongates, while the other, C–O₂, shortens. Despite the relatively small variations in the nuclear skeleton, substantial variations are observed for atomic charges and for the

Table 1. Experimental and Calculated Polarizabilities of CO₂ in Cubic Atomic Units (au³)

	α_{\parallel}	α_{\perp}	$\langle\alpha\rangle$	$\kappa = (\alpha_{\parallel} - \alpha_{\perp})/3\alpha$	$\Delta\alpha = \alpha_{\parallel} - \alpha_{\perp}$
expt. ³⁴	27.250	13.018	17.76	0.267	14.232
calculated	26.024	12.750	17.17	0.258	13.274

dipole moment (see Figures S1 and S2 in the Supporting Information (SI)). The variations of charges, bond orders, and dipole moment are a consequence of the polarizability of the electronic cloud that adjusts to the external stimulus: the π electrons density rearranges more markedly, leaving the σ -bonds almost unaffected (see Table 2). Most of the variables of Table 2 show linear variations with respect to the field intensity.

The superlinear behavior of the polarizability with the electric field can be understood if one considers that in a sum-over-state model, the polarizability tensor elements are expressed as

$$\alpha_{ij} = \sum_k \frac{\langle 0|x_i|k\rangle\langle k|x_j|0\rangle}{\Delta E_{0k}} \quad (1)$$

where $\langle 0|$ represents the ground state wave function, $|k\rangle$ is the wave function of the k th excited state, and ΔE_{0k} is their energy gap. The field affects the molecular wave functions, both in the ground and in the excited states, together with the energy gaps. Variations of the denominator in eq 1 result in the presence of resonances and therefore nonlinearity in the response. The question arises whether the response is dominated by a single quantity, such as the variation of the energy of one orbital.

Figures 1 and 2 show that the lowest unoccupied molecular orbital (LUMO) is affected the most by the field. The energy variation of the occupied orbitals with the field is relatively modest. The LUMO energy can be described by a parabolic function, with a correlation coefficient of 0.998:

$$E_{\text{LUMO}} = a + bF + cF^2 \quad (2)$$

where E_{LUMO} is the energy of the orbital in electron volts, F is the electric field in volts per nanometer, $a = -0.2871$, $b = -0.13417$, and $c = -0.0033124$, in the appropriate units.

The LUMO behavior is at odds with that of the highest occupied molecular orbital (HOMO), whose energy can simply be fitted to a linear equation with the field. Crossing of the two functions occurs at 41.91 V/nm,³⁸ where HOMO and LUMO become degenerate, and the quantum chemical calculation does not converge.

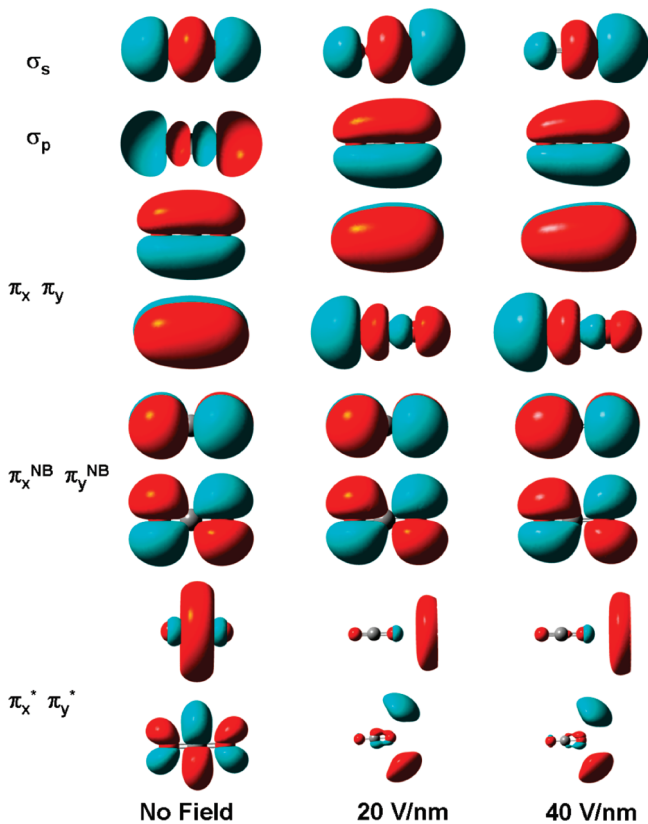
Figure 2 shows that at 40 V/nm the LUMO is localized to the right of the elongating CO bond.

Closing of the HOMO–LUMO gap promotes the spontaneous detachment of the oxygen atom and the formation of two fragments. Indeed, in the calculations, at fields higher than 40 V/nm, the molecule spontaneously breaks down.

Also important is the exchange of positions of the two π_x and π_y orbitals with the σ_p orbital. While the σ_s orbital is stabilized by the EEF, the additional node present in σ_p makes the orbital more susceptible to an increase of the strength of the field. The inversion makes the new orbital distribution

Table 2. Bond Lengths (Å), Atomic Charges, Dipole Moment (debyes), Polarizability (au³), and Bond Orders for C–O₁ and C–O₂ Bonds at Various Field Strengths (V/nm)

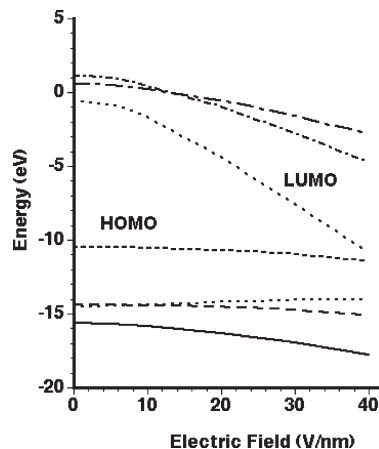
field intensity	C–O ₁	C–O ₂	charge on C	charge on O ₁	charge on O ₂	μ	$\alpha_{ }$	bond order C–O ₁	bond order C–O ₂
0	1.160	1.160	0.38	−0.19	−0.19	0.00	26.024	1.90	1.90
5	1.168	1.154	0.38	−0.25	−0.13	0.72	26.093	1.83	1.93
10	1.176	1.148	0.39	−0.32	−0.07	1.46	26.317	1.77	2.02
20	1.194	1.139	0.43	−0.47	0.04	2.95	27.329	1.64	2.15
30	1.216	1.132	0.48	−0.64	0.16	4.56	29.770	1.52	2.28
40	1.245	1.128	0.53	−0.86	0.33	6.45	38.882	1.40	2.41


Figure 1. Evolution of frontier MOs of CO₂ molecule as a function of the field applied. Occupied orbitals are drawn at a contour value of 0.02 au, while unoccupied orbitals are drawn at a contour value of 0.004 au.

similar to that of a CO orbital fragment localized on C=O₂ atoms and O₁ atom, further promoting the breaking of the C=O₁ bond.

The quadratic variation of the LUMO energy can be explained in terms of second-order Stark effect. The first order one does not appear in molecules. The more polarizable an MO, the larger its energy variation.³⁷ The results imply a substantial polarizability of the LUMO, which is of great consequence for CO₂ reactivity in the presence of electric fields.

In the absence of the field, previous *ab initio* calculations³⁹ of the stationary points on the potential energy surfaces of the lowest singlet and triplet of CO₂, and their crossing, showed that the unimolecular decomposition of CO₂ can proceed via a spin-forbidden channel and has to go through a singlet–triplet crossing, CO₂ → O(³P) + CO. The spin-allowed


Figure 2. Frontier orbital energies in CO₂ as a function of the field applied.

decomposition of CO₂ → CO + O(¹D) is much higher in endothermicity.

Experimentally, the most energetically favorable channel of CO₂ decomposition has an endothermicity of 5.45 eV.⁴⁰ Our calculations (Figure S3 in the SI) in the absence of external field resulted in 5.43 eV, vouching further for the accuracy of the calculations.

The calculations also found that the barrier to decompose CO₂, i.e., the transition state of the reaction, coincides with the crossing between the singlet and triplet state and is located at 5.9 eV, with a C–O₁ bond length of 1.94 Å.

The presence of an external field of 20 V/nm makes the reaction exoergic. The barrier to decompose the molecule is lowered to 5.4 eV. The geometry of the crossing between the curves of different spin multiplicity is characterized by a C–O₁ bond length of 2.20 Å. Increasing the field to 40 V/nm enhances these effects. The barrier is lowered to 3.17 eV, and the reaction becomes extremely exoergic by more than 20 eV. The three-point extrapolation of the energies of the transition states as a function of the field with a quadratic function would give 56.6 V/nm as the intensity required for the spontaneous breaking of the carbon–oxygen bond. The extrapolation does not take into account the dramatic rearrangement of the electronic wave function that takes place when the HOMO and LUMO become degenerate.

The species that originate from the splitting of the CO₂ molecule vary in charge as a function of the field. Up to 10 V/nm, neutral O and CO fragments form. At fields greater than 30 V/nm O₁ is a dianion, while CO is a dication. At intermediates

Table 3. Atomic Charges of CO and O₁ Fragments at Various Field Strengths (V/nm) after Splitting (10 Å for 0, 5, 10, 20, 30 V/nm and 8 Å for 40 V/nm)

field intensity	charge on O ₁	charge on C	charge on O ₂
0	0.0	0.14	-0.14
5	0.0	0.09	-0.09
10	0.0	0.05	-0.05
20	-1.0	0.69	0.31
30	-2.0	1.03	0.96
40	-2.0	1.01	0.99

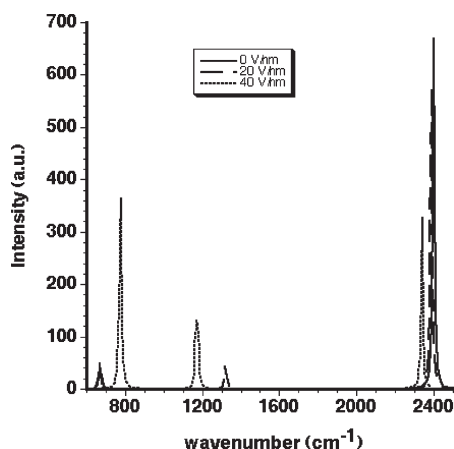


Figure 3. Molecular vibrational Stark effect: calculated IR spectrum of CO₂ at different field strengths.

fields, O₁ is an anion while CO is a cation, (see Table 3). The species formed at higher fields are highly reactive, and their evolution can account for the formation of carbonaceous material found experimentally. The bottleneck of the process is the activation and splitting of the very stable CO₂ molecule.

Alternative splitting pathways involving CO₂⁺ or CO₂⁻ can be excluded. The simple presence of voltage either produced by the AFM tip or by asperities cannot produce anions, which are extremely difficult to generate experimentally in the gas phase. The voltage and the associated field can still rip an electron off CO₂. However, the calculated energy profiles for CO₂⁺ splitting have higher barriers than for the neutral species (see Supporting Information).

To monitor the dissociation dynamics in the presence of the field, infrared spectroscopy can be used. In the experiments, after the capture of CO₂ in the gap region between the two electrodes, the electric field polarizes the carbon dioxide molecule, and the resulting dipole moment interacts with the field. The action of the field is on the time scale of electronic motions, and its effects are not hindered by nearby molecules so that the alignment is quantitative and extremely fast. Figure 3 presents the results of the vibrational Stark effect. The inactive infrared band of the symmetric stretching appears in the spectrum. At 0 V/nm it is calculated as inactive and located at 1369 cm⁻¹, at 20 V/nm it is downshifted to 1323 cm⁻¹, while at 40 V/nm it is further downshifted to 1174 cm⁻¹. Analogously, the bending vibration goes from 674 cm⁻¹ at 0 V/nm, to 668 cm⁻¹ at 20 V/nm, to 778 cm⁻¹ at 40 V/nm.

Also the frequency variations are superlinear and if detected they could be used to assess the field intensity.

To recapitulate, quantum chemical calculations show that CO₂ can spontaneously break in the presence of an electric field above 40 V/nm. The process was present in recent experiments carried out with AFM at room temperature in the presence of low-to-moderate voltages (~10–40 V).²⁵ The rupture occurs at the intersection of the potential energy curves of the singlet and triplet manifolds. It is caused by the fast decrease of the energy of the LUMO that is extrapolated to become degenerate with the HOMO at 41.91 V/nm. Infrared spectroscopy could be used to monitor the field-dependent splitting of CO₂.

SUPPORTING INFORMATION AVAILABLE Variation of atomic charges, dipole moments, and ionization potentials calculated at increasing field strength. Potential energy diagrams for unimolecular decomposition of CO₂ and CO₂⁺ calculated at the B3LYP/aug-cc-PVTZ level of theory at 0, 20, 40 V/nm. Detailed comparison of the energies at B3LYP/aug-cc-PVTZ and CCSD(T)/aug-cc-PVTZ levels at 20 and 40 V/nm. Cartesian Coordinates of a CO₂ molecule optimized under EEF. This material is available free of charge via the Internet at <http://pubs.acs.org>.

AUTHOR INFORMATION

Corresponding Author:

*To whom correspondence should be addressed. E-mail: matteo.calvaresi@studio.unibo.it (M.C.); francesco.zerbetto@unibo.it (F.Z.).

REFERENCES

- (1) Franzen, S.; Goldstein, R. F.; Boxer, S. G. Electric Field Modulation of Electron Transfer Reaction Rates in Isotropic Systems: Long-Distance Charge Recombination in Photosynthetic Reaction Centers. *J. Phys. Chem.* **1990**, *94*, 5135–5149.
- (2) Lao, K.; Franzen, S.; Stanley, R. J.; Lambright, D. G.; Boxer, S. G. Effects of Applied Electric Fields on the Quantum Yields of the Initial Electron-Transfer Steps in Bacterial Photosynthesis. 1. Quantum Yield Failure. *J. Phys. Chem.* **1993**, *97*, 13165–13171.
- (3) Murgida, D. H.; Hildebrandt, P. Electron-Transfer Processes of Cytochrome *c* at Interfaces. New Insights by Surface-Enhanced Resonance Raman Spectroscopy. *Acc. Chem. Res.* **2004**, *37*, 854–861.
- (4) Aittala, P. J.; Cramariuc, O.; Hukka, T. I. Electric-Field-Assisted Electron Transfer in a Porphine–Quinone Complex: A Theoretical Study. *J. Chem. Theory Comput.* **2010**, *6*, 805–816.
- (5) Töbik, J.; Dal Corso, A.; Scandolo, S.; Tosatti, E. Organic Molecular Crystals in Electric Fields. *Surf. Sci.* **2004**, *566*–568, 644–649.
- (6) Leung, K.; Rempe, S. B.; Schultz, P. A.; Sproviero, E. M.; Batista, V. S.; Chandross, M. E.; Medforth, C. J. Density Functional Theory and DFT+U Study of Transition Metal Porphines Adsorbed on Au(111) Surfaces and Effects of Applied Electric Fields. *J. Am. Chem. Soc.* **2006**, *128*, 3659–3668.
- (7) Harikumar, K. R.; Polanyi, J. C.; Sloan, P. A.; Ayissi, S.; Hofer, W. A. Electronic Switching of Single Silicon Atoms by Molecular Field Effects. *J. Am. Chem. Soc.* **2006**, *128*, 16791–16797.
- (8) Reed, M. A.; Zhou, C.; Muller, C. J.; Burgin, T. P.; Tour, J. M. Conductance of a Molecular Junction. *Science* **1997**, *278*, 252–254.

- (9) Chen, J.; Reed, M. A.; Rawlett, A. M.; Tour, J. M. Large On–Off Ratios and Negative Differential Resistance in a Molecular Electronic Device. *Science* **1999**, *286*, 1550–1552.
- (10) Blum, A. S.; Kushmerick, J. G.; Long, D. P.; Patterson, C. H.; Yang, J. C.; Henderson, J. C.; Yao, Y.; Tour, J. M.; Shashidhar, R.; Ratna, B. R. Molecularly Inherent Voltage-Controlled Conductance Switching. *Nat. Mater.* **2005**, *4*, 167–172.
- (11) Alemani, M.; Peters, M. V.; Hecht, S.; Rieder, K.-H.; Moresco, F.; Grill, L. Electric Field-Induced Isomerization of Azobenzene by STM. *J. Am. Chem. Soc.* **2006**, *128*, 14446–14447.
- (12) Shaik, S.; de Visser, S. P.; Kumar, D. External Electric Field Will Control the Selectivity of Enzymatic-Like Bond Activations. *J. Am. Chem. Soc.* **2004**, *126*, 11746–11749.
- (13) Hirao, H.; Chen, H.; Carvajal, M. J.; Wang, Y.; Shaik, S. Effect of External Electric Fields on the C–H Bond Activation Reactivity of Nonheme Iron–Oxo Reagents. *J. Am. Chem. Soc.* **2008**, *130*, 3319–3327.
- (14) Meir, R.; Chen, H.; Lai, W.; Shaik, S. Oriented Electric Fields Accelerate Diels–Alder Reactions and Control the Endo/Exo Selectivity. *ChemPhysChem* **2010**, *11*, 301–310.
- (15) Harada, A.; Kataoka, K. Switching by Pulse Electric Field of the Elevated Enzymatic Reaction in the Core of Polyion Complex Micelles. *J. Am. Chem. Soc.* **2003**, *125*, 15306–15307.
- (16) Lai, W.; Chen, H.; Cho, K.-B.; Shaik, S. External Electric Field Can Control the Catalytic Cycle of Cytochrome P450_{cam}: A QM/MM Study. *J. Phys. Chem. Lett.* **2010**, *1*, 2082–2087.
- (17) Choi, Y. C.; Kim, W. Y.; Park, K.-S.; Tarakeshwar, P.; Kim, K.-S. Role of Molecular Orbitals of the Benzene in Electronic Nanodevices. *J. Chem. Phys.* **2005**, *122*, 094706.
- (18) Li, Y.; Zhao, J.; Yin, X.; Yin, G. Ab Initio Investigations of the Electric Field Dependence of the Geometric and Electronic Structures of Molecular Wires. *J. Phys. Chem. A* **2006**, *110*, 11130.
- (19) Rai, D.; Joshi, H.; Kulkarni, A. D.; Gejji, S. P.; Pathak, R. K. Electric Field Effects on Aromatic and Aliphatic Hydrocarbons: A Density-Functional Study. *J. Phys. Chem. A* **2007**, *111*, 9111–9121.
- (20) Garcia, R.; Martinez, R. V.; Martinez, J. Nano-Chemistry and Scanning Probe Nanolithographies. *Chem. Soc. Rev.* **2006**, *35*, 29–38.
- (21) Tello, M.; Garcia, R.; Martín-Gago, J. A.; Martínez, N. F.; Martín-González, M. S.; Aballe, L.; Baranov, A.; Gregoratti, L. Bottom-Up Fabrication of Carbon-Rich Silicon Carbide Nanowires by Manipulation of Nanometer-Sized Ethanol Menisci. *Adv. Mater.* **2005**, *17*, 1480–1483.
- (22) Suez, I.; Backer, S. A.; Frechet, J. M. J. Generating an Etch Resistant “Resist” Layer from Common Solvents Using Scanning Probe Lithography in a Fluid Cell. *Nano Lett.* **2005**, *5*, 321–324.
- (23) Kinser, C. R.; Schmitz, M. J.; Hersam, M. C. Kinetics and Mechanism of Atomic Force Microscope Local Oxidation on Hydrogen-Passivated Silicon in Inert Organic Solvents. *Adv. Mater.* **2006**, *18*, 1377–1380.
- (24) Suez, I.; Rolandi, M.; Backer, S. A.; Scholl, A.; Doran, A.; Okawa, D.; Zettl, A.; Frechet, J. M. J. High-Field Scanning Probe Lithography in Hexadecane: Transitioning from Field Induced Oxidation to Solvent Decomposition through Surface Modification. *Adv. Mater.* **2007**, *19*, 3570–3573.
- (25) Garcia, R.; Losilla, N. S.; Martinez, J.; Martinez, R. V.; Palomares, F. J.; Huttel, Y.; Calvaresi, M.; Zerbetto, F. Nanopatterning of Carbonaceous Structures by Field-Induced Carbon Dioxide Splitting with a Force Microscope. *App. Phys. Lett.* **2010**, *96*, 143110.
- (26) Weast, E. R. C. *Handbook of Chemistry and Physics*; CRC Press: Boca Raton, FL, 1991.
- (27) Seinfeld, J.; Pandis, S. N. *Atmospheric Chemistry and Physics*; John Wiley & Sons: Hoboken, NJ, 2006 (and references therein).
- (28) Pradier, J. P.; Pradier, C. M. *Carbon Dioxide Chemistry: Environmental Issues*; The Royal Society of Chemistry: Cambridge, 1994.
- (29) Frisch, M. J.; Trucks, G. W.; Schlegel, H. B.; Scuseria, G. E.; Robb, M. A.; Cheeseman, J. R.; Montgomery, Jr., J. A.; Vreven, T.; Kudin, K. N.; Burant, J. C. et al. *Gaussian 03*, revision E.01; Gaussian, Inc.: Wallingford, CT, 2004.
- (30) Becke, A. D. Density-Functional Thermochemistry. III. The Role of Exact Exchange. *J. Chem. Phys.* **1993**, *98*, 5648–5652.
- (31) Lee, C.; Yang, W.; Parr, R. G. Development of the Colle–Salvetti Correlation-Energy Formula into a Functional of the Electron Density. *Phys. Rev. B* **1988**, *37*, 785–789.
- (32) Stephens, P. J.; Devlin, F. J.; Chabalowski, C. F.; Frisch, M. J. Ab Initio Calculation of Vibrational Absorption and Circular Dichroism Spectra Using Density Functional Force Fields. *J. Phys. Chem.* **1994**, *98*, 11623–11627.
- (33) Dunning, T. H., Jr. Gaussian Basis Sets for Use in Correlated Molecular Calculations. I. The Atoms Boron through Neon and Hydrogen. *J. Chem. Phys.* **1989**, *90*, 1007–1023.
- (34) Pople, J. A.; Head-Gordon, M.; Raghavachari, K. Quadratic Configuration Interaction. A General Technique for Determining Electron Correlation Energies. *J. Chem. Phys.* **1987**, *87*, 5968–5975.
- (35) Bridge, N. J.; Buckingham, A. D. The Polarization of Laser Light Scattered by Gases. *Proc. R. Soc., Ser. A* **1966**, *295*, 334–349.
- (36) Lewis, M.; Wu, Z.; Glaser, R. Polarizabilities of Carbon Dioxide and Carbodiimide. Assessment of Theoretical Model Dependencies on Dipole Polarizabilities and Dipole Polarizability Anisotropies. *J. Phys. Chem. A* **2000**, *104*, 11355–11361.
- (37) Kim, W. Y.; Kim, K. S. Tuning Molecular Orbitals in Molecular Electronics and Spintronics. *Acc. Chem. Res.* **2010**, *43*, 111–120.
- (38) The energies of the HOMO and LUMO were fitted by quadratic functions that cross each other at 41.91 V/nm.
- (39) Hwang, D.-Y.; Mebel, A. M. Ab Initio Study of Spin-Forbidden Unimolecular Decomposition of Carbon Dioxide. *Chem. Phys.* **2000**, *256*, 169–176.
- (40) Herzberg, G. *Molecular Spectra and Molecular Structure: III. Electronic Structure of Polyatomic Molecules*; Van Nostrand: New York, 1966; pp 589, 604.